



## Direct numerical simulation of fluid flow and heat transfer in periodic wavy channels with rectangular cross-sections

Y. Sui, C.J. Teo <sup>\*</sup>, P.S. Lee

Department of Mechanical Engineering, National University of Singapore, 9 Engineering Drive 1, Singapore 117576, Singapore

### ARTICLE INFO

#### Article history:

Received 18 March 2011

Received in revised form 22 August 2011

Accepted 22 August 2011

Available online 21 September 2011

#### Keywords:

Microchannel heat sinks

Electronic cooling

Wavy microchannel

Chaotic advection

Dean vortices

Dynamical system

Poincaré section

Ruelle-Takens-Newhouse

### ABSTRACT

Fully-developed flow and heat transfer in periodic wavy channels with rectangular cross sections are studied using direct numerical simulation, for increasing Reynolds numbers spanning from the steady laminar to transitional flow regimes. The results show that steady flow is characterized by the formation of symmetric secondary flow or Dean vortices when liquid flows past the bends. It is found that the patterns of Dean vortices may evolve along the flow direction, thus leading to chaotic advection, which can greatly enhance the convective fluid mixing and heat transfer. With increasing Reynolds numbers, the flow undergoes transition from a steady state to a periodic one with a single frequency, and subsequently to a quasiperiodic flow with two incommensurate fundamental frequencies. Within these unsteady regimes, the flow is characterized by very complex Dean vortices patterns which evolve temporally and spatially along the flow direction, and the flow symmetry may even be lost. Further increase in Reynolds number leads to chaotic flow, where the Fourier spectrum of the velocity evolution becomes broadband. The bifurcation scenario in wavy channels may thus share some common features with the well-known Ruelle-Takens-Newhouse scenario. Heat transfer simulation in all flow regimes is carried out with constant wall temperature condition and liquid water as the coolant. It is found that due to the efficient mixing in wavy channels, the heat transfer performance is always significantly more superior to that of straight channels with the same cross sections; at the same time the pressure drop penalty of wavy channels can be much smaller than the heat transfer enhancement. The present study shows that these wavy channels may have advantages over straight channels and thus serve as promising candidates for incorporation into efficient heat transfer devices.

© 2011 Elsevier Ltd. All rights reserved.

## 1. Introduction

In recent years, with the miniaturization of coolant flow-through heat transfer devices, approaches by which heat transfer performance can be improved without large pressure drop penalties or inducing complicated three-dimensional structures which renders the fabrication very challenging have become a subject of increased interest. Due to the reduced size of heat exchangers, high flow rates of the coolant will culminate in a sharp increase in pressure loss. Turbulent convective heat transfer, which is an efficient mode of heat transfer, is not viable. The flow of the coolant through mini heat exchangers is in the laminar or possibly transitional regimes. Convective heat transfer depends significantly on fluid mixing. Flow mechanisms which can enhance fluid mixing and thus improve heat transfer are an important research field and have driven a considerable number of theoretical, numerical and experimental studies.

One promising flow mechanism for enhancing heat transfer involves the use of Dean vortices. When liquid flows through curved passages, secondary flows (Dean vortices) may be generated due to centrifugal forces. The secondary flows promote rotation of fluid elements in the spanwise plane of the curved passage, which in turn enhances the stretching and folding of the fluid elements, thus improving the mixing as well as heat transfer. This mechanism has been employed by many researchers for mixers [1,2] and heat transfer enhancement [3–6].

Recently, Fletcher and coworkers [7–11] have systematically performed numerical studies of fully-developed flow and heat transfer in periodic serpentine channels with various cross-section shapes. Their simulations focused mainly on the steady laminar flow regime. It has been found that Dean vortices and more complex vertical flow patterns emerge when the liquid coolant flows through the bends. The heat transfer performance could be greatly enhanced over straight channels with the same cross section; at the same time the pressure drop penalty is much smaller than the heat transfer enhancement. Manglik et al. [12] numerically investigated the steady and laminar forced convection in wavy-plate-fin channels under periodically developed air flow conditions. Their

\* Corresponding author. Tel.: +65 6516 8037.

E-mail address: [mpeteocj@nus.edu.sg](mailto:mpeteocj@nus.edu.sg) (C.J. Teo).

## Nomenclature

$A$	heat conduction area	$T_w$	wall temperature
$A_c$	channel cross-section area	$U$	average flow velocity
$c_p$	specific heat	$x$	$x$ -coordinate
$D$	hydraulic diameter	$y$	$y$ -coordinate
$E_f$	pressure drop penalty factor	$z$	$z$ -coordinate
$E_{Nu}$	heat transfer enhancement factor		
$f$	friction factor		
$h$	average heat transfer coefficient		
$H$	channel depth		
$k$	thermal conductivity		
$L$	wavelength of one wavy unit		
$Nu$	Nusselt number		
$p$	static pressure		
$q''$	heat flux		
$Pr$	Prandtl number		
$Re$	Reynolds number		
$S$	channel width		
$T$	oscillation period		
$T_{x,y,z}$	local fluid temperature		
$T_m$	mean (bulk) fluid temperature		

<i>Greek symbols</i>	
$\alpha$	dimensionless channel width
$\beta$	channel cross-section aspect ratio
$\phi$	rotation angle
$\mu$	fluid viscosity
$\rho$	fluid density

<i>Subscripts</i>	
$c$	channel
$f$	pressure drop penalty factor
$m$	mean
$nu$	heat transfer enhancement factor
$w$	wall
$x$	local

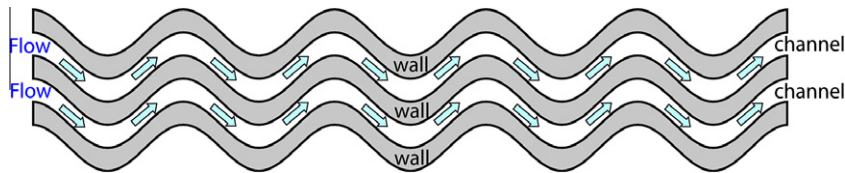


Fig. 1. Illustration of planar sinusoidal channels for microchannel heat sinks.

three-dimensional simulation results revealed symmetric Dean vortex pairs in the cross sections of the sinusoidal channels. Significant heat transfer enhancement, as well as pressure drop penalty, had been observed.

The present authors have previously proposed to improve the performance of microchannel heat sinks by replacing the conventionally employed straight channels with sinusoidal channels, as shown in Fig. 1. They have numerically investigated liquid-water flow and heat transfer in three-dimensional wavy microchannels with rectangular cross sections [13]. The simulation results showed that secondary flow (Dean vortices) developed and the heat transfer performance of the wavy microchannels was much more superior than that of straight channels with the same cross section; at the same time, the pressure drop penalty could be much smaller than the heat transfer enhancement. This general conclusion has subsequently been confirmed experimentally by the present authors [14]. In the experiments, flow friction and heat transfer in wavy microchannels fabricated on copper blocks were studied with deionized water as the coolant. Gong et al. [15] recently performed parametric numerical studies of flow and heat transfer in wavy microchannels, and it was found that for certain wavy geometries the overall performance of wavy channels can still be much better than that of straight channels, even at intermediate Reynolds number where Dean vortices are not present.

In the authors' previous numerical simulation work [13], to explain the heat transfer enhancement, the flow field was investigated and the dynamical system technique (Poincaré sections) was employed to analyze the fluid mixing. It was found that the quantity and the location of the Dean vortices may change significantly along the flow direction, which can lead to chaotic advection. It is well known that chaotic advection can greatly improve convective fluid mixing and thus enhance heat transfer.

The present authors also attempted to explain how the spatial evolution of Dean vortex could lead to chaotic advection using Aref's theoretical model of blinking vortex [16,17]. However, as the wavy microchannels considered in the previous study [13,14] consist of only ten sinusoidal units, the flow may be far from fully-developed and thus the developing flow effect may have played an important role in fluid mixing and heat transfer. Without the developing flow effect, it is still largely unknown whether chaotic advection and the corresponding heat transfer enhancement still prevail.

For flow in wavy passages, the critical Reynolds number for flow transition can be significantly lower than that in straight channels. Rush et al. [18] have experimentally studied the flow and heat transfer in sinusoidal passages with high aspect ratios. They observed unsteady flow at Reynolds numbers as low as 200. The critical Reynolds number for onset of unsteadiness highly depends on the channel geometry as well as the total channel length in the

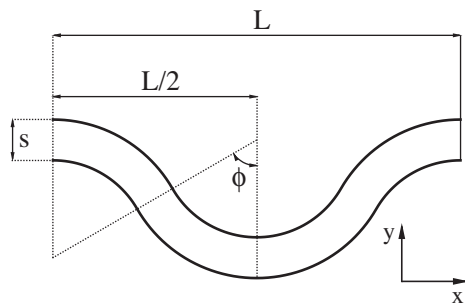
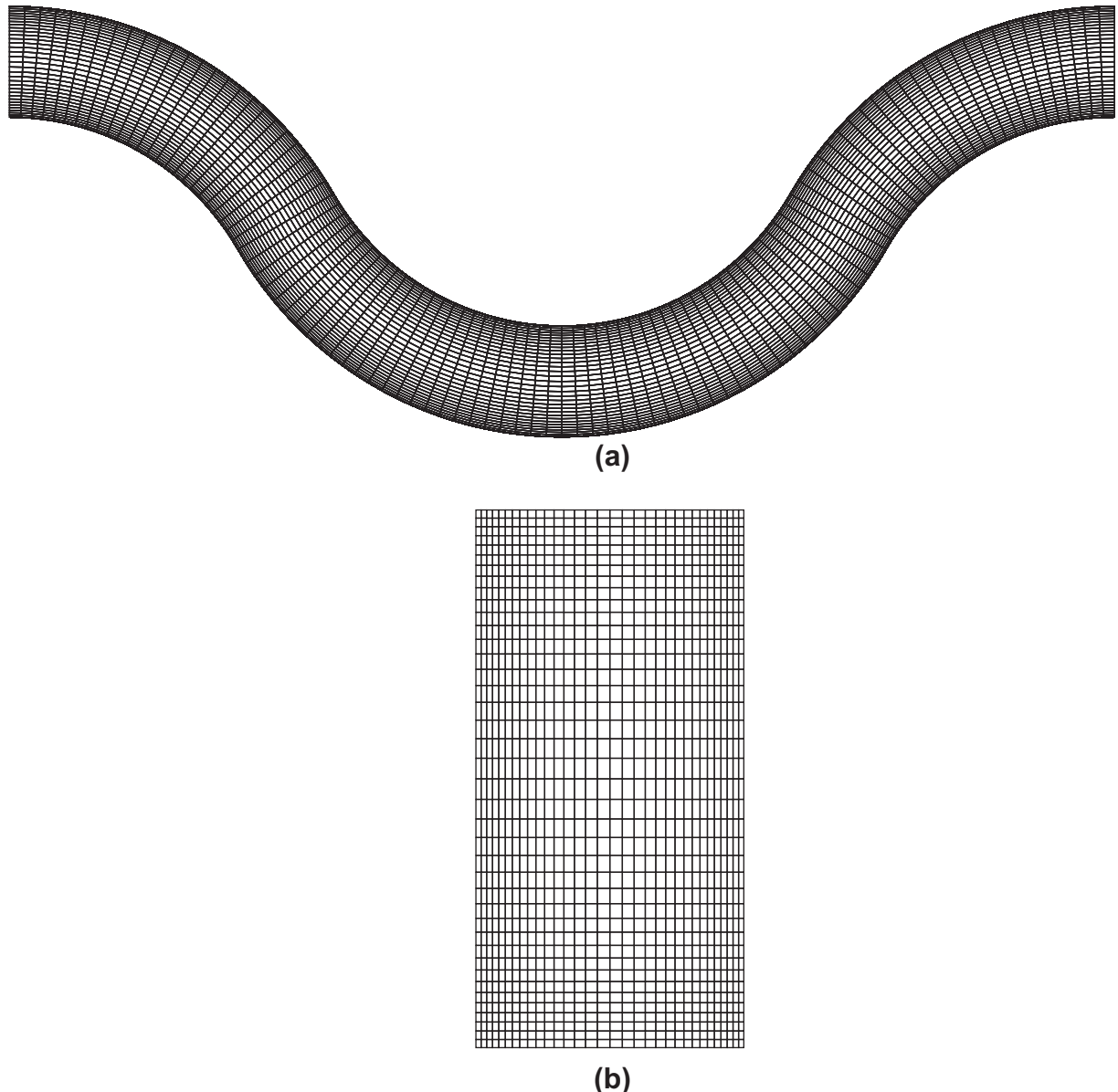


Fig. 2. Characteristic dimensions for one periodic unit of a curved duct.



**Fig. 3.** Illustration of computational mesh for a wavy channel with  $\alpha = 0.1$ ,  $\beta = 1/2$  and  $\varphi = \pi/3$ . Views from (a) x-y; (b) x-z plane.

flow direction. The unsteadiness can be considered as a disturbance to the fluid and may enhance fluid mixing and heat transfer. It is thus very meaningful and important to investigate the unsteady flow and heat transfer in wavy channels. Direct numerical

simulation can provide useful information pertaining to the spatial and temporal evolution of the flow field and the corresponding heat transfer performance. However, most previous computational studies focus on the steady laminar flow regime and the fluid flow and heat transfer in the transitional regime in three dimensional wavy channels is still not well explored, to the best of the authors' knowledge.

In the present study, direct numerical simulation is carried out to investigate the fully-developed flow and heat transfer in periodic wavy channels with rectangular cross sections. The flow regimes cover both steady laminar and transitional flows. In the

**Table 1**

Effects of grid size on the results of a wavy microchannel with  $\alpha = 0.1$ ,  $\beta = 1/2$ ,  $\varphi = \pi/3$  at  $Re = 166.7$ .

Grid size	$U_p$	$fRe$	$Nu_T$
$33 \times 41 \times 101$	1.643	83.18	11.82
$41 \times 51 \times 121$	1.645	83.19	11.76

**Table 2**

Effects of grid size on the results of a wavy microchannel with  $\alpha = 0.1$ ,  $\beta = 1/2$ ,  $\varphi = \pi/3$  at  $Re = 200$ .

Grid size	Time step	$(U_p)_{min}$	$(U_p)_{max}$	$fRe$	$Nu_T$
$33 \times 41 \times 101$	0.02	1.469	1.727	88.51	12.13
$41 \times 51 \times 121$	0.01	1.466	1.734	88.48	12.11

**Table 3**

Comparison of present computational results with theoretical data for a straight channel with  $\beta = 1/2$ .

	$fRe$	$Nu_T$
Present computational results	62.02	3.395
Theoretical results [21]	62.00	3.390

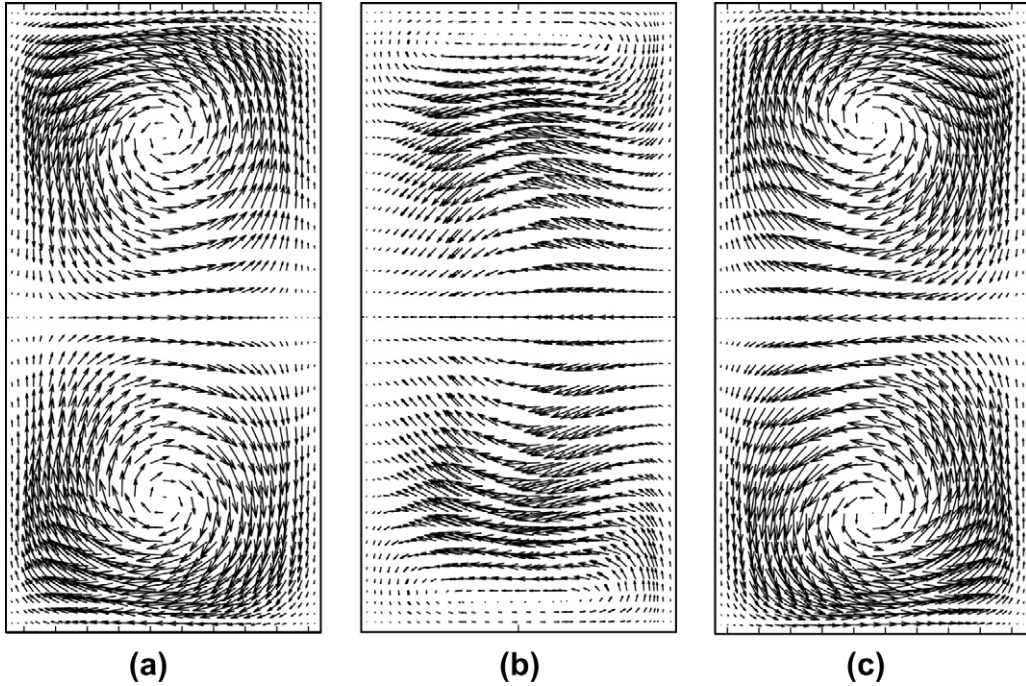


**Fig. 4.** Velocity vectors along cross sections of a wavy channel with  $\alpha = 0.1$ ,  $\beta = 1/2$  and  $\varphi = \pi/3$  at  $Re = 66.67$ . The axial locations of the cross sections are: (a)  $x = 0$ ; (b)  $x_{min} = 0.3L$  and perpendicular to the flow direction; (c)  $0.5L$ .

steady flow regime, the spatial evolution of the flow field is investigated and the dynamical system technique (Poincaré section), as well as stretching field, is employed to analyze the fluid mixing. In the transitional flow regime, both spatial and temporal evolutions of the flow field are studied. Fluid mixing analysis becomes very

difficult for unsteady flow. The temporal evolution of the velocity at certain locations within the wavy channels is recorded and the oscillation frequency is identified by carrying out Fast Fourier Transformation, in an attempt to find out the bifurcation scenario. For all flow regimes, heat transfer simulation is carried out with constant wall temperature conditions and liquid water ( $Pr = 7$ ) is chosen as the coolant. Both the transient and the time averaged heat transfer performance as well as friction loss of the present wavy channels are studied and compared with straight channels

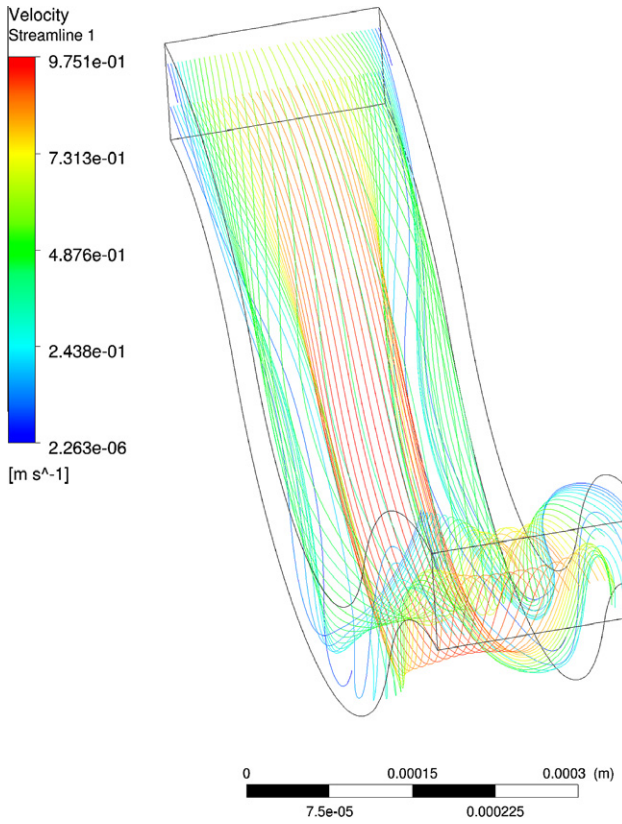


**Fig. 5.** Pathlines showing swirling motion of the fluid in the wavy channel of Fig. 4.

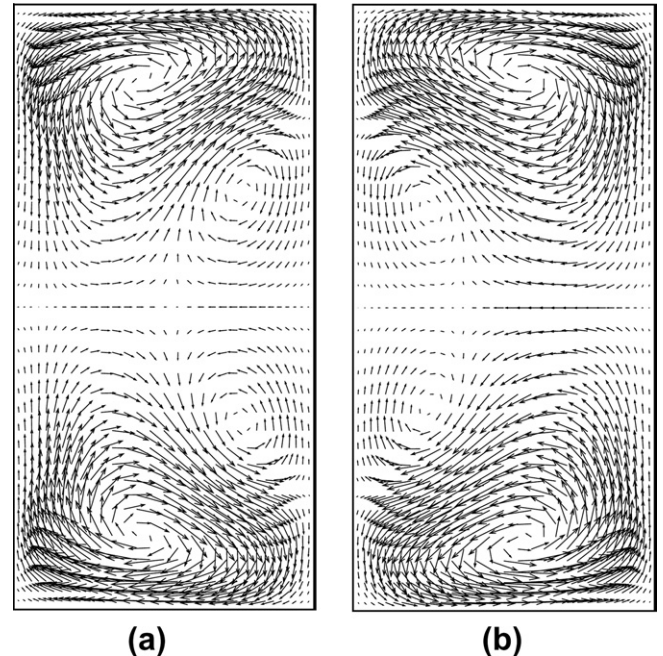


**Fig. 6.** Velocity vectors along cross sections of a wavy channel with  $\alpha = 0.1$ ,  $\beta = 1/2$  and  $\varphi = \pi/3$  at  $Re = 166.7$ . The axial locations of the cross sections are: (a)  $x = 0$  and (b)  $0.5L$ .

with the same cross sections. The heat transfer results are discussed with the flow field analysis.

## 2. Computational method

The characteristic dimensions of a typical wavy channel unit with length  $L$  and depth  $H$  (in  $z$ -direction) is shown in Fig. 2. It is formed by four identical annuli with axial width  $S$  and rotation angle  $\varphi$ . The dimensionless representations of these shape parameters are channel axial width ( $\alpha = S/L$ ), cross-section aspect ratio ( $\beta = S/H$ ) and rotation angle  $\varphi$  which can be treated as a parameter representing the curved amplitude. In the present study, the parameters considered are in the following ranges:  $\alpha = 0.1$ ,

$\beta = 1/3-1$  and  $\varphi = \pi/6-\pi/3$ . The hydraulic and thermal performance of such wavy channels are studied and compared with baseline channels, which have the same cross sections and total lengths as the wavy channels.

The entire computational domain consists of one wavy unit as shown in Fig. 2. The geometry of the wavy channel unit is configured in GAMBIT [19]. The computational domain is meshed with hexahedral volume elements using the Map scheme in Gambit. The computational mesh is relatively uniform in axial direction. In the cross section of the wavy channel, the channel width and depth are meshed with a double successive ratio of 1.05 (in the  $y$ - and  $z$ -directions, the size ratio of two adjacent meshes equals 1.05). Fig. 3 presents the computational mesh for a wavy channel with  $\alpha = 0.1$ ,  $\beta = 1/2$  and  $\varphi = \pi/3$ . The Navier–Stokes equation in

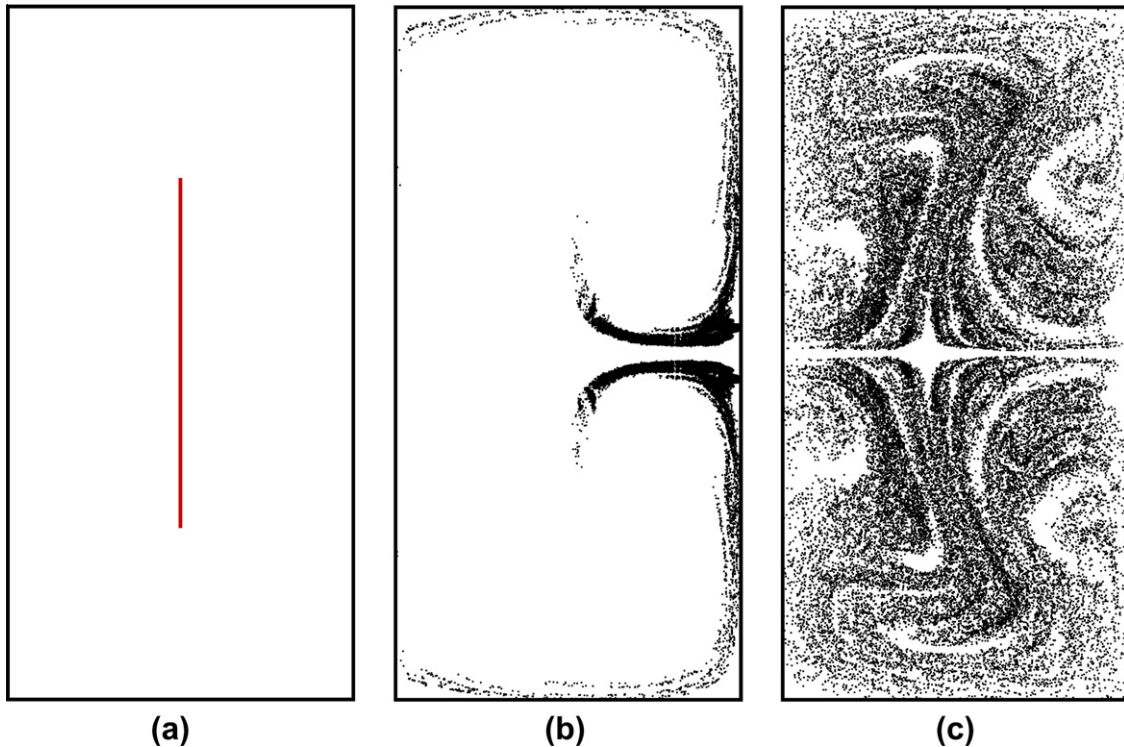


**Fig. 7.** Poincaré sections obtained from particle tracking for a wavy channel with  $\alpha = 0.1$ ,  $\beta = 1/2$  and  $\varphi = \pi/3$  at  $Re =$  (b) 66.67 and (c) 166.7. The red line in (a) shows the initial locations of the 20,000 massless and non-diffusive particles in the channel inlet. (For interpretation of the references to colour in this figure legend, the reader is referred to the web version of this article.)

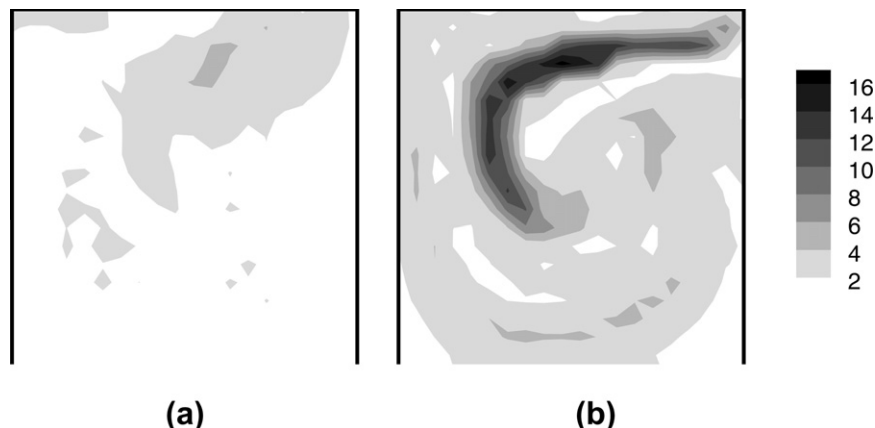


**Fig. 8.** Stretching fields of the cross sections at  $x = 0$  of a wavy channel with  $\alpha = 0.1$ ,  $\beta = 1/2$  and  $\varphi = \pi/3$  at  $Re =$  (a) 66.7 and (b) 166.7 (only the upper half cross sections are shown due to symmetry).

its unsteady, incompressible form is solved using the general-purpose finite-volume based computational fluid dynamics (CFD) software package, FLUENT [20]. Constant fluid properties are assumed in the present simulation. The second-order implicit scheme in FLUENT is used for the temporal discretization. For the spatial discretization, the standard scheme is used for pressure discretization, and the SIMPLE scheme is employed for pressure–velocity coupling. The momentum and energy equations are solved with second-order up-wind scheme. Periodic boundary condition with constant mass flow rates is specified at the inlet and outlet of the channel. No-slip and constant wall temperature conditions are specified on the side walls of the wavy channel. During the time marching process, the computations for each time step are considered to have converged when the residues for continuity and energy decrease to less than  $1 \times 10^{-7}$  and  $1 \times 10^{-10}$ , respectively.

The Reynolds number in the present study is defined as

$$Re = \rho U D / \mu \quad (1)$$

where  $\rho$  is the fluid density,  $U$  is the average flow velocity,  $D$  is the hydraulic diameter and  $\mu$  represents the fluid dynamic viscosity. The transient and time-averaged frictional loss (expressed in terms of a friction factor) and heat transfer performance (quantified by the Nusselt number) of the present wavy channels are computed and compared with straight channels having the same cross sections. The friction factor is defined as:

$$f = -[(dp/dx)(2D/\rho U^2)] \quad (2)$$

The local Nusselt number is defined as:

$$Nu = hD/k \quad (3)$$

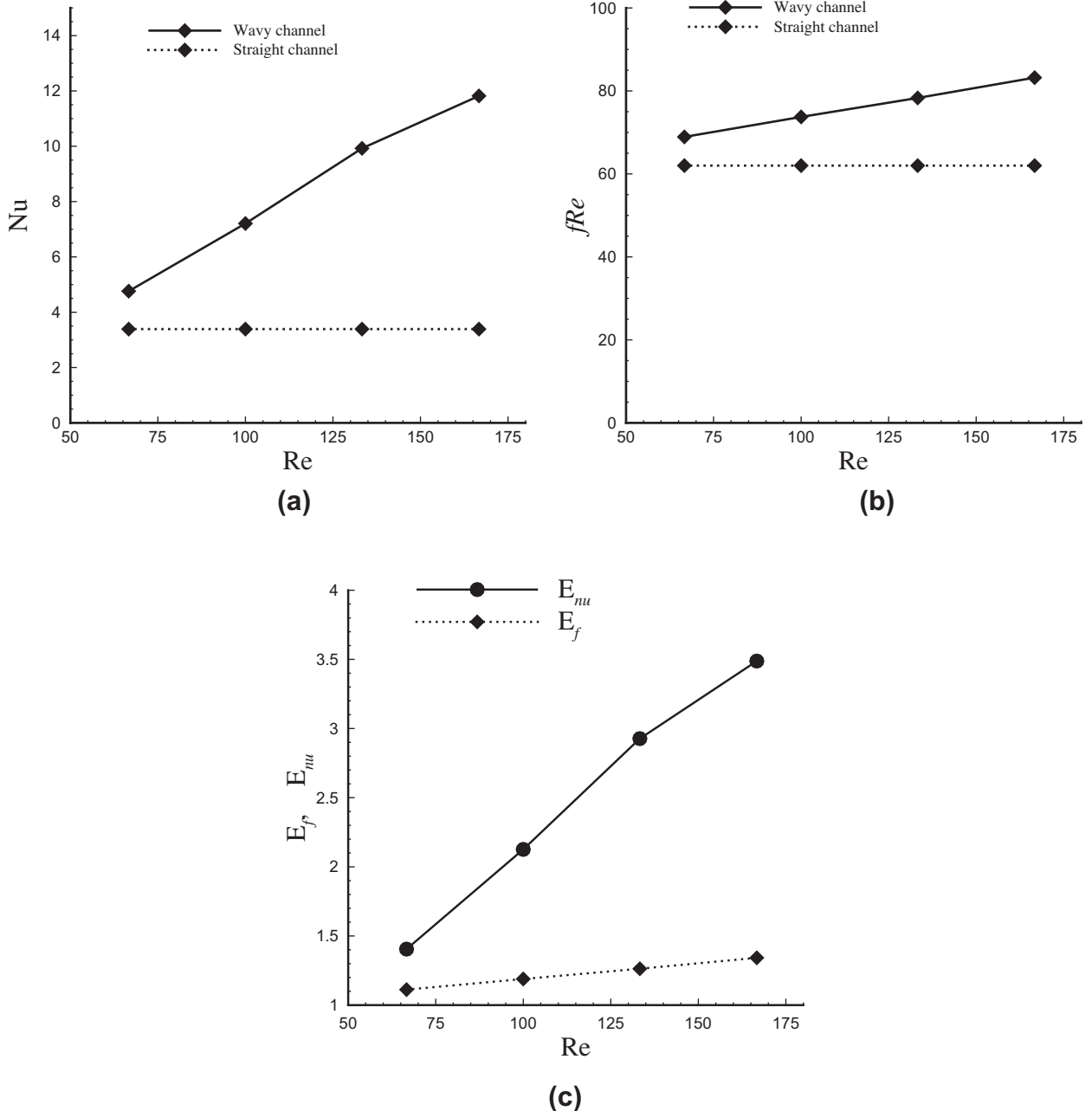


**Fig. 9.** (a)  $Nu$ ; (b)  $fRe$ ; (c) heat transfer enhancement and pressure drop penalty factors for a wavy channel with  $\alpha = 0.1$ ,  $\beta = 1/2$  and  $\varphi = \pi/3$  and a straight baseline channel at different Reynolds numbers.

where  $h$  represents the local heat transfer coefficient and  $k$  is the thermal conductivity of the coolant. The heat transfer coefficient  $h$  is evaluated following the definitions of Shah and London [21]. For simulation under constant wall temperature condition, the heat transfer coefficient is evaluated from:

$$h_x = q'' / \frac{(T_w - T_{m,in}) - (T_w - T_{m,out})}{\ln[(T_w - T_{m,in})/(T_w - T_{m,out})]} \quad (4)$$

where  $T_w$  is the temperature of the conduction wall, and  $T_{m,x}$  represents the local bulk fluid temperature, defined as:

$$T_{m,x} = \left( \int_{A_c} u T_{x,y,z} dA_c \right) / UA_c \quad (5)$$

The terms  $T_{m,in}$  and  $T_{m,out}$  are the bulk fluid temperatures at the inlet and outlet of the wavy channel. The term  $q''$  represents the heat flux, evaluated by:

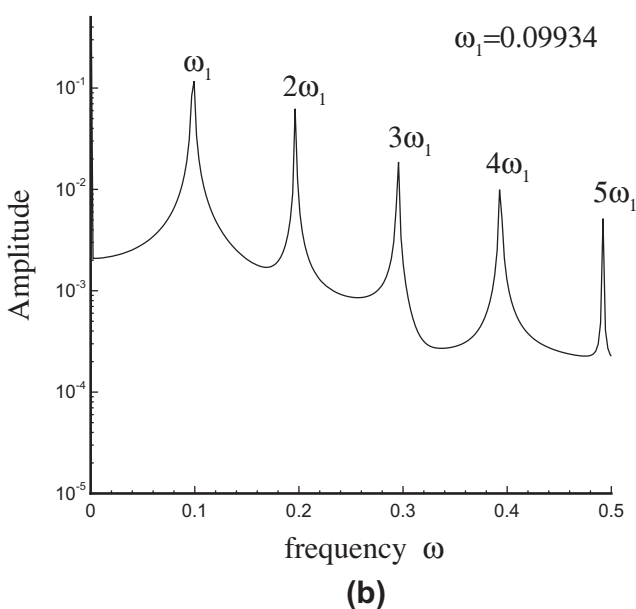
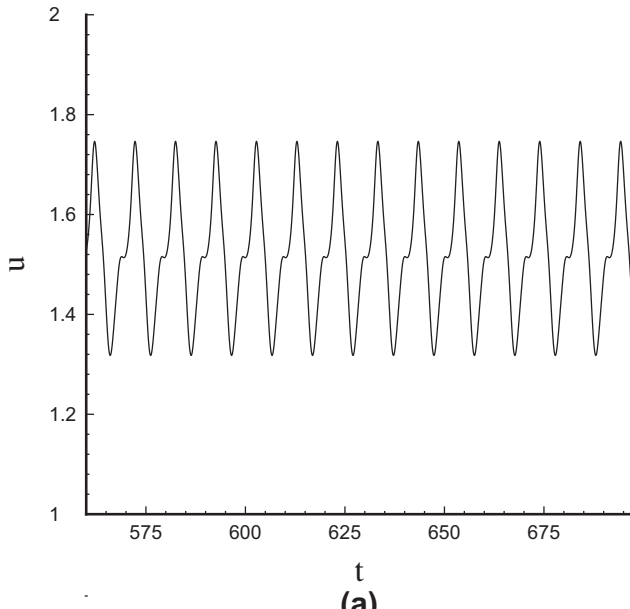


**Fig. 10.** (a) Temporal evolution of the  $x$ -direction component of flow velocity at a certain point (point  $P$ ) which is located at the center of the middle cross section ( $x = 0.5L$ ) of a wavy channel with  $\alpha = 0.1$ ,  $\beta = 1/2$  and  $\varphi = \pi/3$  at  $Re = 233.3$  and (b) Fourier power spectrum of the  $x$ -direction velocity component.

$$q'' = \dot{m}c_p(T_{m,in} - T_{m,out})/A \quad (6)$$

where  $\dot{m}$  represents the mass flow rate,  $c_p$  is the specific heat and the term  $A$  is the total heat conduction area of the side walls. For unsteady simulations, the time-averaged friction factor and Nusselt number are calculated from:

$$f = \int_T f_t dt / T \quad (7)$$

$$Nu = \int_T Nu_t dt / T \quad (8)$$

where the integration time  $T$  represents the oscillation period.

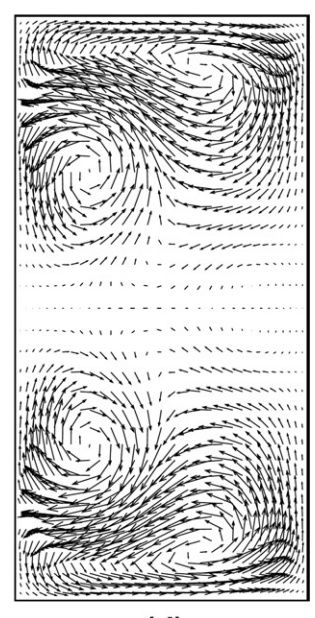
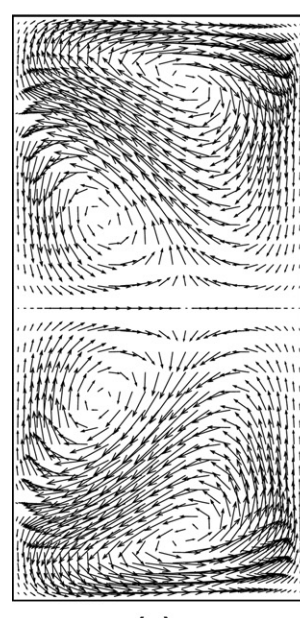
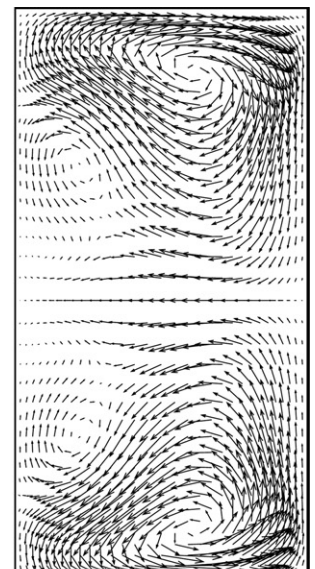
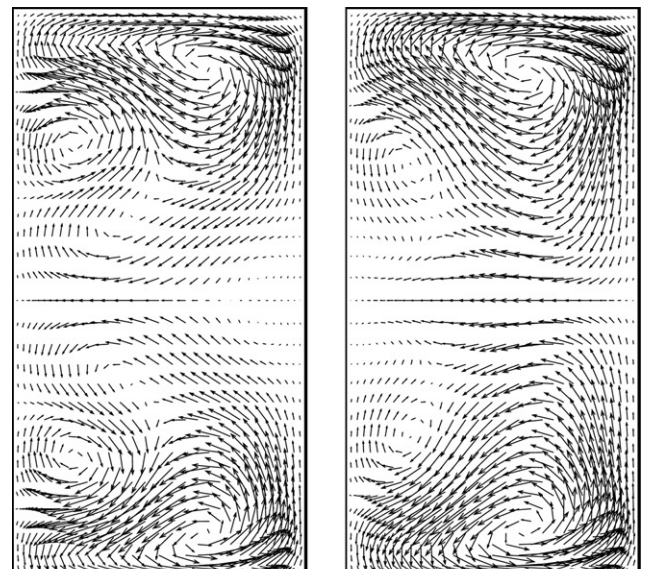


**Fig. 11.** Instantaneous velocity vectors along the middle cross section ( $x = 0.5L$ ) of a wavy channel with  $\alpha = 0.1$ ,  $\beta = 1/2$  and  $\varphi = \pi/3$  at  $Re = 233.3$ . (a)  $t = 0$ ; (b)  $t = 2/7T$ ; (c)  $t = 4/7T$  and (d)  $t = 6/7T$ .

### 3. Results and discussion

The first series of simulations is carried out for selecting the most optimal grid. A typical wavy channel geometry with  $\alpha = 0.1$ ,  $\beta = 1/2$  and  $\varphi = \pi/3$  is chosen as the test case. The grid independence study covers both the steady and periodic flow regimes. In the steady regime, the  $x$ -component of the flow velocity at a certain point (point  $P$ ) which is located at the center of the middle cross section ( $x = 0.5L$ ) of the wavy channel, the overall  $fRe$  and Nusselt number are chosen as indicators. For the periodic flow regime, the maximum and minimum of the velocity component in the  $x$ -direction of the same point within one oscillation period, the time averaged overall  $fRe$  and Nusselt number are chosen as the indicators. After successive grid refinement experiments, the final selected mesh size is 33 points in channel width direction, 41 points in channel depth direction and 101 points in axial direction. The mesh size is further increased from  $33 \times 41 \times 101$  to  $41 \times 51 \times 121$ , and the simulation results for  $Re = 167$  which falls into the steady flow regime are presented in Table 1. It can be seen that the relative error is within 0.5% which indicates that the mesh density is sufficient for steady flow simulation. For the periodic flow regime, numerical simulation is carried out at  $Re = 200$  for the two sets of mesh using different time steps. In the present study, the hydraulic diameter  $D$  is chosen to be the length scale and  $D/U$  is the time scale. The length and time in the present study are all normalized by the corresponding scales. The results for  $Re = 200$  are presented in Table 2. With the grid refinement from  $33 \times 41 \times 101$  to  $41 \times 51 \times 121$  and time step refinement from 0.02 to 0.01, the indicator variables only change by less than 0.4%, which may indicate that the mesh size and time step are sufficient for capturing important unsteady flow characteristics. Such a mesh size and time step are employed for simulation of wavy channels with geometrical parameters  $\alpha = 0.1$ ,  $\beta = 1/3-1/2$  and  $\varphi = \pi/6-\pi/3$ . For wavy channels with aspect ratio of  $\beta = 1$ , the same time step is employed with a slightly different grid size of  $33 \times 33 \times 101$ .

To validate the numerical model, the approach of Manglik et al. [12] has been adopted: simulations are carried out for a channel with  $\alpha = 0.1$ ,  $\beta = 1/2$  and  $\varphi = 0$ , which is actually a straight channel and the analytical results for  $fRe$  and  $Nu$  can be found in the

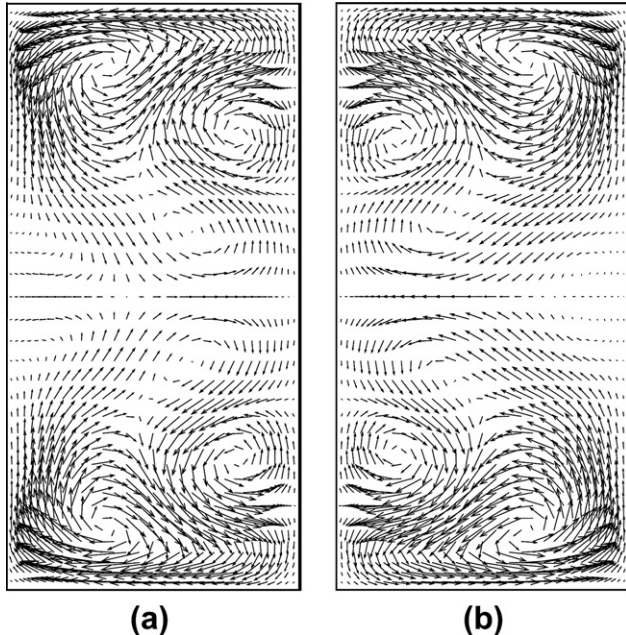


**Fig. 12.** Instantaneous velocity vectors along cross sections of a wavy channel with  $\alpha = 0.1$ ,  $\beta = 1/2$  and  $\varphi = \pi/3$  at  $Re = 233.3$  and  $t = 0$ . The axial locations of the cross sections are:  $x =$  (a) 0 and (b)  $0.5L$ .

classical book of Shah and London [21]. The results of the present simulation are compared with the analytical results in Table 3. It can be seen that the differences are within 0.15%. Another independent validation of the present method can be found in a recent work performed by the present authors [14]: the same numerical method has been employed to study the flow friction and heat transfer in wavy channels consisting of ten wavy units, and experiments have been conducted based on similar conditions. The simulation results regarding the flow friction and heat transfer have been found to agree favorably with the experimental data.

#### 3.1. Steady flow regime

At low Reynolds numbers, the flow field in wavy channels can be characterized as steady with a symmetric pair of counter rotating secondary vortices in the cross section of the channel, which

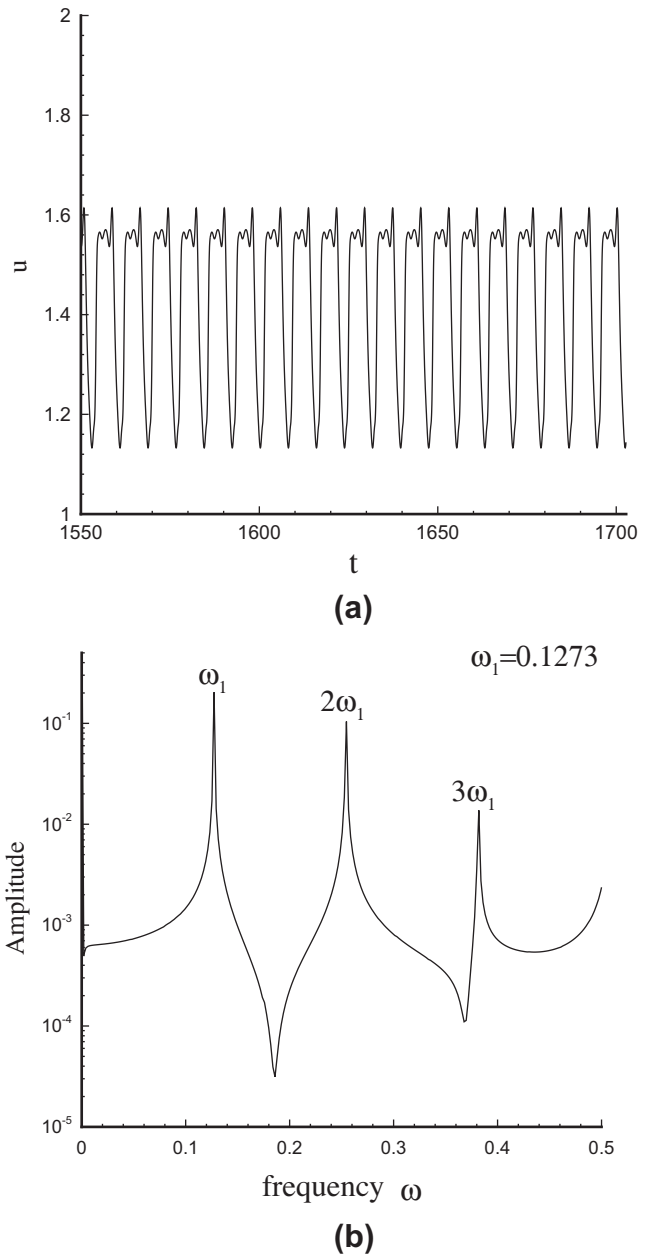


**Fig. 13.** (a) Temporal evolution of the  $x$ -component of flow velocity at the point  $P$  of a wavy channel with  $\alpha = 0.1$ ,  $\beta = 1/2$  and  $\varphi = \pi/3$  at  $Re = 266.7$ . (b) Fourier power spectrum of the  $x$ -direction velocity component.

can be seen from Fig. 4 for a wavy channel with  $\alpha = 0.1$ ,  $\beta = 1/2$  and  $\varphi = \pi/3$  at  $Re = 66.67$ . The secondary vortices promote rotation of fluid elements in the spanwise plane of the channel and make the flow helical, which can be observed in Fig. 5 from the pathlines of massless particles released at the channel inlet. The centers of the vortices shift to the upper and lower walls of the channel with increasing Reynolds numbers. For a wavy channel with given geometry, there is a qualitative change in flow pattern when the Reynolds number exceeds a critical value. As can be seen from Fig. 6, which depicts results for the same channel as Fig. 4, at a higher Reynolds number of 166.7, Dean vortices have developed and there are multiple symmetric pairs of secondary vortices. Thus it can be expected that the fluid elements in the wavy channels will trace out very complex helical flow patterns.

It is more interesting when the secondary flow evolution along the flow direction is investigated. From Fig. 4, it can be observed that the secondary flow patterns in the cross sections of the wavy channel at  $x = 0$  and  $x = 0.5L$  are similar as only the rotation reverses its direction. In the plane perpendicular to the bulk flow direction at approximately  $x = 0.3L$ , the vortex is less pronounced since this plane is in close proximity to the location where the curvature switches sign. Significant changes in flow pattern can be seen in Fig. 6. From  $x = 0$  to  $x = 0.5L$ , Dean vortices have shifted from the right wall to the left wall. Recently it has been found by Schönfeld and Hardt [1], Jiang et al. [2] as well as the present authors [13] that change in secondary flow patterns along the flow direction can lead to chaotic advection. However, developing flow was considered in all studies and thus may partly account for the spatial evolution of the secondary flow patterns. The developing flow effect has been ruled out as fully-developed flow is considered in the present study. Actually, the curvature of the wavy channel periodically switches sign, which causes the centrifugal force sustained by the fluid to periodically change direction when fluid flows through the channel, thus culminating in the spatial evolution of flow patterns. The spatial evolution of secondary flow patterns also depends strongly on Reynolds number as they are essentially inertia induced flow.

To analyze fluid mixing, particle tracing simulation is carried out to elucidate the advection of non-diffusive and massless tracer particles in the flow, as adopted by some other researchers [2,22,23]. After the velocity field reaches a steady state, tracer particles are released from certain locations. The instantaneous location of each tracer particle can be obtained by time integration using a second-order Runge–Kutta scheme via the following equation:

$$\mathbf{x}(t) = \int_0^t \mathbf{u}(\mathbf{x}(t')) dt' \quad (9)$$

The instantaneous velocity of a tracer particle can be evaluated by spatial interpolation using the fluid velocities of the surrounding Eulerian mesh points. Here a Taylor series expansion and least squares based method [24] is employed which can achieve second order accuracy. After the particles' path lines are known, their positions at any cross sectional plane along the microchannel can be easily obtained by interpolation. As the velocity field is periodic at the inlet and outlet of the channel, the present particle tracking simulation takes advantage of this periodicity and extends the results to practical channels consisting of many periodic wavy units. This is achieved by setting the cross sectional position of a tracer particle at the channel unit outlet as the position at the inlet of an adjacent channel unit. In the present study, Poincaré sections are generated by tracking 20,000 tracers, which are initially evenly distributed along a straight line in the cross section at the channel inlet (position shown in red in Fig. 7(a)), through the channel for 10 periods (units) and recording their cross-sectional positions at the outlet. Fig. 7 presents the Poincaré sections for a wavy channel with  $\alpha = 0.1$ ,  $\beta = 1/2$  and  $\varphi = \pi/3$  at  $Re = 66.67$  and 166.7. It is known that for fully-developed flow in straight channels, the streamlines of the coolant are straight. Thus Fig. 7(a) can be also be considered as the Poincaré section for a straight channel with  $\alpha = 0.1$ ,  $\beta = 1/2$ . It can be seen from Fig. 7(b) for  $Re = 66.67$  that most area of the cross section is devoid of tracer points, which indicates poor mixing. However for  $Re = 166.7$ , there is strong stretching and folding of fluid material line and the tracer particles which are initially along

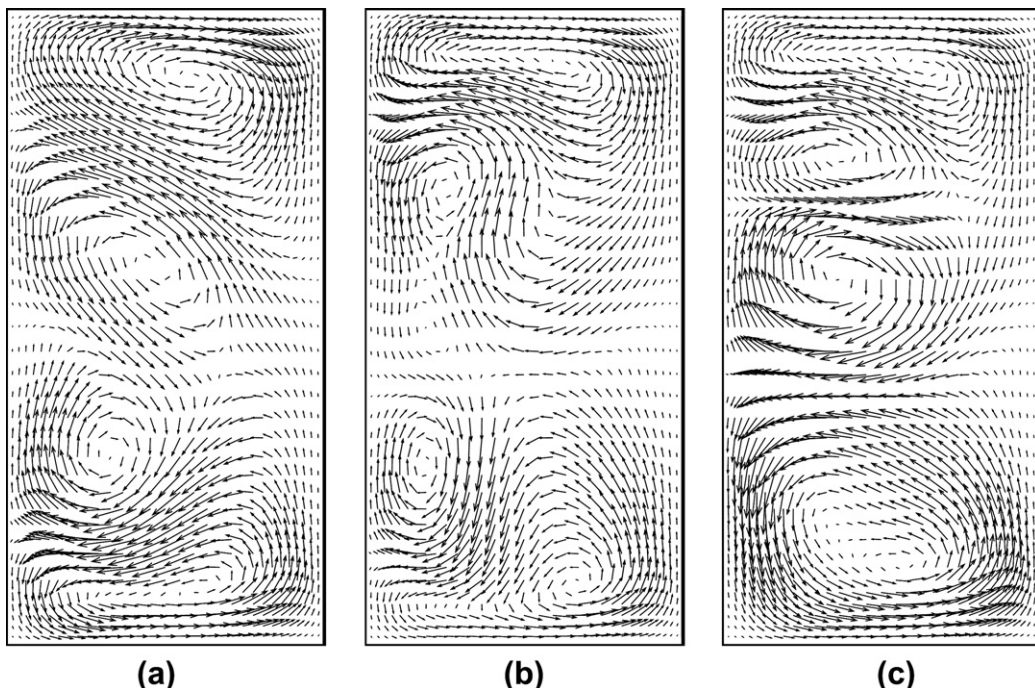


**Fig. 14.** Instantaneous velocity vectors along the middle cross section ( $x = 0.5L$ ) of a wavy channel with  $\alpha = 0.1$ ,  $\beta = 1/2$  and  $\varphi = \pi/3$  at  $Re = 266.7$ . (a)  $t = 0$ ; (b)  $t = 1/3T$  and (c)  $t = 2/3T$ .

a straight line have covered almost the whole area of the cross section, which is a signature of chaotic advection [15,25,26]. Together with the flow field results of Figs. 4 and 6 and the discussion, it may be found that chaotic advection strongly depends on the secondary flow pattern evolution along the flow direction. In fact, Aref [16] theoretically studied a two dimensional fluid stirred by a point vortex and found that when the vortex periodically changes its location between two different positions, chaotic advection can be generated and the fluid becomes well mixed. The spatial change of secondary flow patterns in the present wavy channels share some similar features with those of Aref, as the periodic spatial dimension in the present flow is analogous to the periodic time dimension in the two dimensional flow of Aref. That may account for the chaotic advection observed in the present wavy channels.

It is well known that chaotic advection can be generated in two-dimensional unsteady flow or three-dimensional steady flow. In the steady laminar flow regime, in order to generate chaotic advection for enhancing mixing or heat transfer, three-dimensional multi-layer channels or complicated structures are always needed to stretch and fold the fluid elements [27–31]. The planar wavy channels in the present study can be considered as a very simple device, in which chaotic advection can be generated even in the steady laminar flow region. In other words, a steady Eulerian flow field in three-dimensions may culminate in a chaotic flow field when analyzed from the Lagrangian viewpoint.

Poincaré sections for straight and wavy channels presented in Fig. 7 can be considered as a qualitative indicator for fluid mixing. In an attempt to quantitatively characterize the local fluid mixing, stretching fields for the wavy channel at different Reynolds numbers are computed, following an approach similar to that of Xia et al. [29]. A pair of non-diffusive and massless tracer particles, with initial separation  $\delta(0)$  close to the minimum mesh size, is released at a certain location  $\mathbf{x}$  in the channel inlet cross section ( $x = 0$ ). After one wavy channel unit, their separation becomes  $\delta(L)$  at section  $x = L$ . The stretching ratio for the location  $\mathbf{x}$  is computed from  $\lambda_{\mathbf{x}} = \delta(L)/\delta(0)$ . From the results in Fig. 8, it is seen that strong stretching is always associated with spanwise vortex. The maximum values of stretching ratio for  $Re = 66.7$  and  $166.7$  are 4.6 and 17.1, respectively. From the stretching field, it is also evident that the stretching extent for  $Re = 166.7$  is significantly higher than that for  $Re = 66.7$ , which suggests better mixing.

With the enhanced mixing in wavy channels compared with straight channels having the same cross section, it can be expected that there will also be heat transfer enhancement. Heat transfer simulation is carried out with constant wall temperature condition and liquid water ( $Pr = 7$ ) chosen as the coolant. The simulation results, in terms of  $Nu$ ,  $fRe$ ,  $E_{Nu}$  and  $E_f$  are presented in Fig. 9 at different Reynolds numbers. The heat transfer enhancement ( $E_{Nu}$ ) and pressure-drop penalty ( $E_f$ ) are defined as the Nusselt number and friction factor of the present wavy channels divided by those of straight baseline channels, respectively [11,13]:

$$E_f = \frac{f_{wavy}}{f_{straight}}, \quad E_{Nu} = \frac{Nu_{wavy}}{Nu_{straight}} \quad (10)$$

From Fig. 9(a) and (b), it can be seen that for all cases considered, the present wavy microchannels are capable of improving the heat transfer performance, albeit with an increase in pressure drop. From Fig. 9(c), it can be found that the heat transfer augmentation can be moderately or significantly larger than the pressure drop penalty throughout the range studied. At  $Re = 66.67$ , there is no chaotic advection; the fluid mixing is relatively weak and is mainly achieved by the fluid elements' rotation induced by the symmetric pair of secondary vortices. The heat transfer performance is boosted up by 40.5% with a pressure drop penalty increase of 11.2%. Both  $E_{Nu}$  and  $E_f$  increase corresponding to an increase in Reynolds number. At

$Re = 166.7$ , chaotic advection is obviously present, which greatly enhances fluid mixing and thus the heat transfer performance and pressure drop penalty increase by 248.8% and 34.2%, respectively, compared with the straight baseline channel.

### 3.2. Unsteady flow regime

It has been clearly established in the previous section that three-dimensional flows with a steady Eulerian flow field may result in chaotic advection, and thus mixing and heat transfer enhancement. It may be envisaged that an unsteady three dimensional Eulerian flow field may potentially culminate in further enhancements in chaotic advection, mixing and heat transfer. In this section, the flow through wavy channels with an unsteady Eulerian flow field will be analyzed in detail.

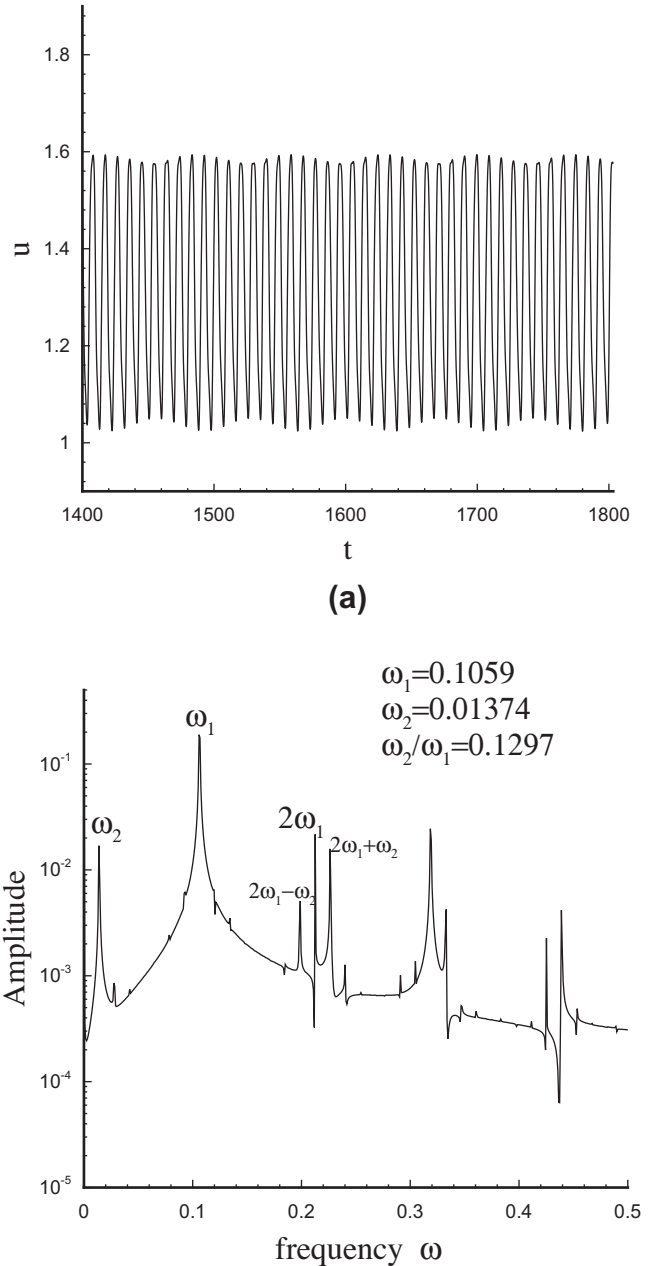


**Fig. 15.** (a) Temporal evolution of the  $x$ -component of flow velocity at the point  $P$  of a wavy channel with  $\alpha = 0.1$ ,  $\beta = 1/2$  and  $\varphi = \pi/3$  at  $Re = 333.3$ . (b) Fourier power spectrum of the  $x$ -direction velocity component.

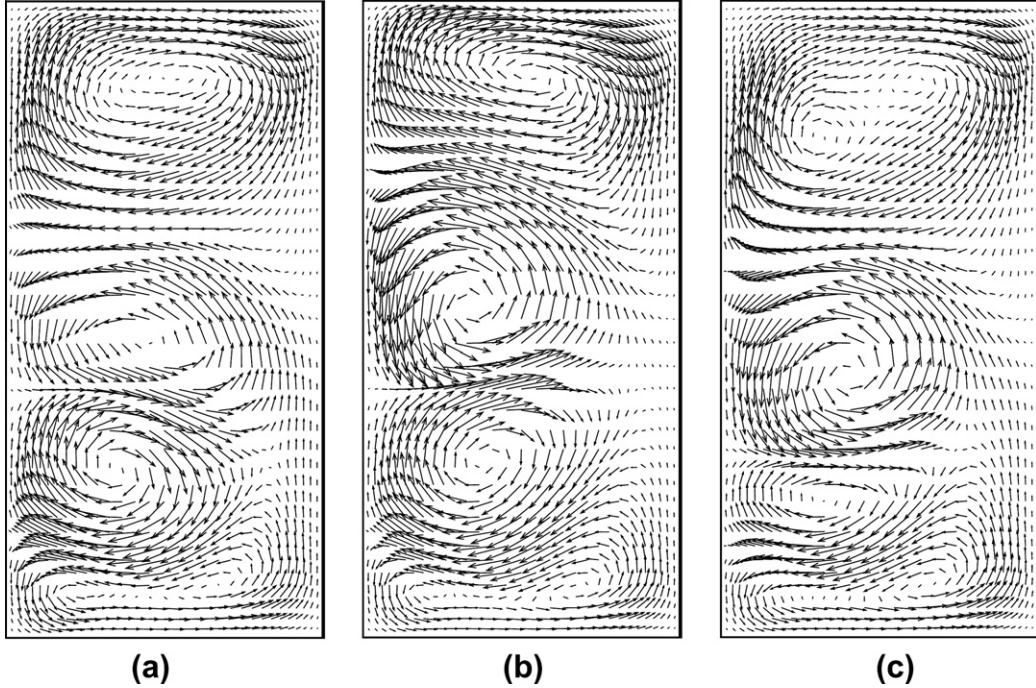


**Fig. 16.** Instantaneous velocity vectors along the middle cross section ( $x = 0.5L$ ) of a wavy channel with  $\alpha = 0.1$ ,  $\beta = 1/2$  and  $\varphi = \pi/3$  at  $Re = 333.3$ . (a)  $t = 0$ ; (b)  $t = 1/3T$  and (c)  $t = 2/3T$ .

With further increase in Reynolds number, the flow in wavy channels transits from steady to time periodic regime via a Hopf bifurcation. The simulation results presented here mainly correspond to a wavy channel with  $\alpha = 0.1$ ,  $\beta = 1/2$  and  $\varphi = \pi/3$ . However, the results are found to be typical and capable of representing the flow evolution scenarios in wavy channels with  $\alpha = 0.1$ ,  $\beta = 1/3-1$  and  $\varphi = \pi/6-\pi/3$  considered in the present study. Fig. 10(a) presents the temporal evolution of the  $x$ -direction component of flow velocity at a particular point at  $Re = 233.3$ . This point, named  $P$  in the present study, is located at the center of the middle cross section ( $x = 0.5L$ ) of a wavy channel. Fast Fourier Transformation is carried out for the velocity evolution and the Fourier power spectrum is presented in Fig. 10(b). From the results, it is obvious that the flow is in the periodic regime with a single frequency. In fact, such analysis methodology has been widely employed for flow transition scenario studies [32–35]. The onset of unsteadiness increases the dimension of the system and makes it more complex. It could be considered as an additional disturbance to the fluid and may enhance mixing. Previous unsteady simulations of two-dimensional converging-diverging channels [33] and grooved channels [34] revealed that the transition of flow from steady to time-dependent and periodic self-sustained regime lead to enhancement in heat transfer rate with only a moderate increase in pressure drop. The temporal evolution of the flow field along the middle cross section ( $x = 0.5L$ ) of the wavy channel is investigated and the instantaneous velocity vector fields at different instants within one oscillation period are presented in Fig. 11 for  $Re = 233.3$ . The symmetric pair of Dean vortices, which attach to the left wall in the figure, are found to periodically change their locations and shapes. Fig. 12 presents the instantaneous velocity vectors along the inlet ( $x = 0$ ) and middle cross section ( $x = 0.5L$ ) of the wavy channel at the same Reynolds number during the time instant  $t = 0$  of Fig. 12. It can be found that the spatial evolution of the secondary flow appears similar to that of Fig. 6 corresponding to the steady flow regime. The spatial and temporal evolution of the flow patterns in the wavy channel may behave like “ghost stirrers” which render the fluid well-mixed. For the present three-

dimensional unsteady flow in wavy channels, carrying out particle tracking simulation, as in Section 3.1 for steady flow, becomes very difficult. It is almost impossible in the present study due to limitations of the commercial software FLUENT employed. However, based on the findings for steady flow in wavy channels, the additional temporal evolution of the flow field is more likely to facilitate the generation of chaotic advection, which will in turn lead to better mixing and heat transfer performance. For time-dependant flow, the flow state is usually characterized by recording the time evolution of a velocity component at a certain

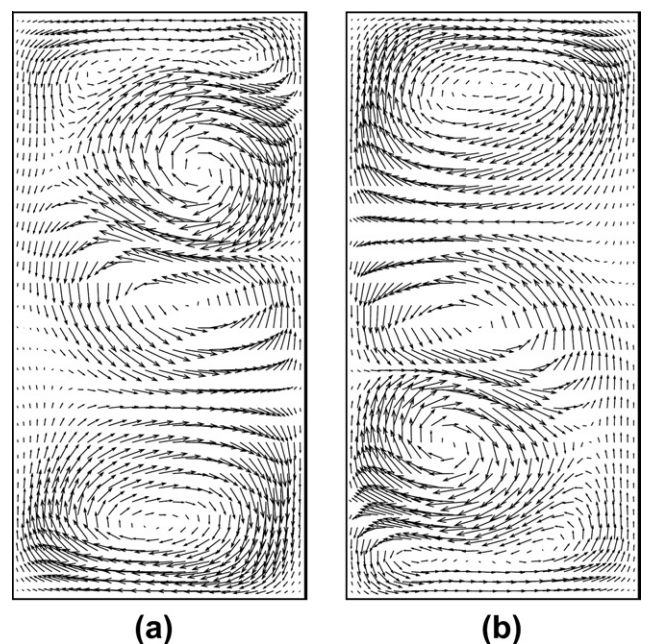
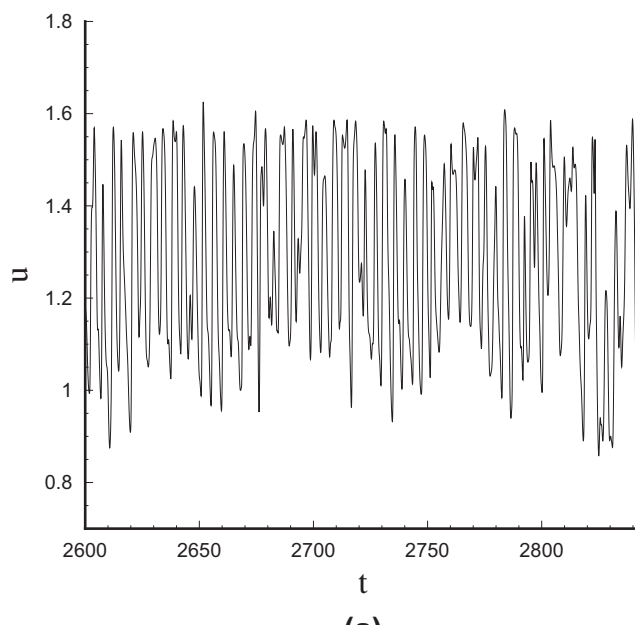


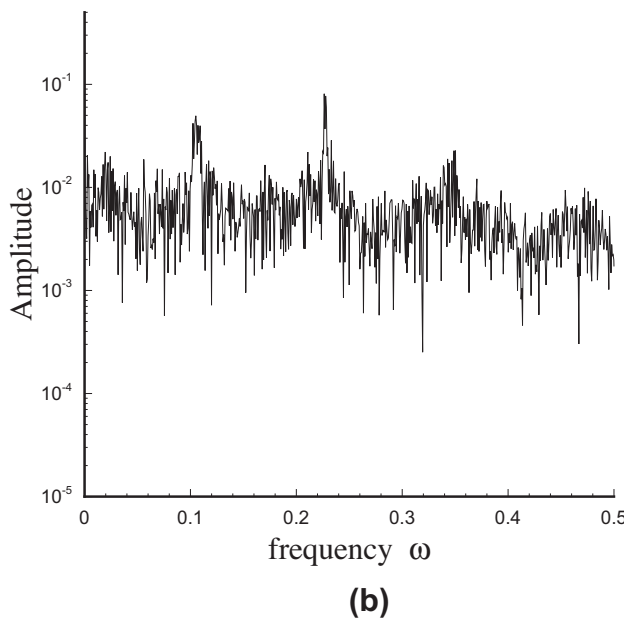
**Fig. 17.** Instantaneous velocity vectors along cross sections of a wavy channel with  $\alpha = 0.1$ ,  $\beta = 1/2$  and  $\varphi = \pi/3$  at  $Re = 333.3$  and  $t = 0$ . The axial locations of the cross sections are:  $x =$  (a)  $0$  and (b)  $0.5L$ .

location within the fluid domain and investigating the Fourier power spectra, as employed in the present study. With further increase in Reynolds number, the flow remains in the periodic regime with one single frequency, as can be found from Fig. 13 for  $Re = 266.7$ . The temporal and spatial evolution of the secondary flow patterns is found to persist. One interesting and qualitative change in flow pattern is that the flow field, which is symmetric about the geometrically symmetric plane ( $x$ - $y$  plane at  $z = 0.5H$ ) at lower Reynolds numbers, loses its symmetry as can be observed from Fig. 14.

For the wavy channel with  $\alpha = 0.1$ ,  $\beta = 1/2$  and  $\varphi = \pi/3$ , qualitative change in the temporal evolution of velocity at point  $P$  occurs for Reynolds number between 300 and 333.3. Fig. 15 presents the temporal evolution for the flow velocity and its Fourier power spectral density. It can be seen that that the flow has undergone



(a)

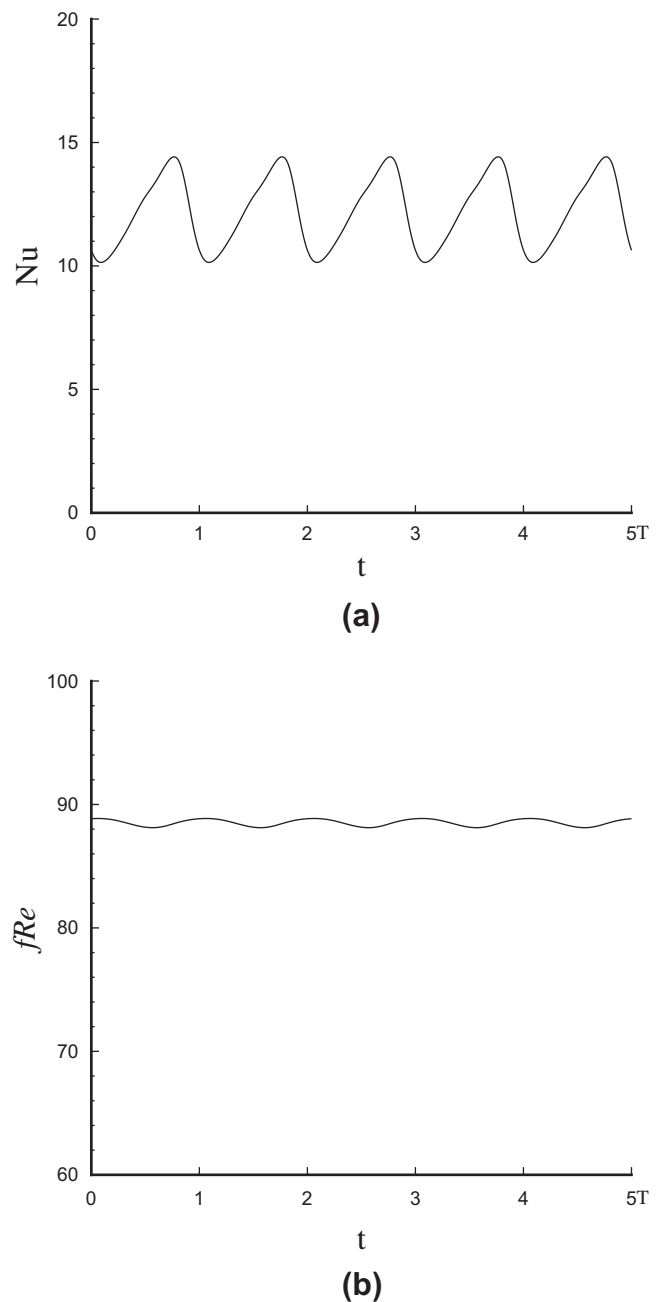


(b)

**Fig. 18.** (a) Temporal evolution of the  $x$ -component of flow velocity at the point  $P$  of a wavy channel with  $\alpha = 0.1$ ,  $\beta = 1/2$  and  $\varphi = \pi/3$  at  $Re = 400$ . (b) Fourier power spectrum of the  $x$ -direction velocity component.

transition into the two-frequency quasiperiodic regime via a second Hopf bifurcation. The spectral peaks shown in Fig. 15(b) correspond to linear combinations of the two fundamental frequencies  $mf_1 + nf_2$ , where  $m$  and  $n$  are integers. The winding number  $f_2/f_1$  is irrational. Fig. 16 presents the time evolution of the flow field along the middle cross section of the wavy channel within the long period corresponding to  $f_2$ . Fig. 17 presents the flow field along the inlet and middle cross sections of the wavy channel at the same Reynolds number corresponding to the instantaneous time of  $t = 0$ . The flow evolution seems qualitatively similar to that of the single frequency periodic regime.

For the same wavy channel, when the Reynolds number is increased above 366.7, an aperiodic behavior appears, as can be seen from Fig. 18. The time evolution of the velocity component and the continuous broadband power spectrum clearly depict the chaotic



(a)

(b)

**Fig. 19.** Temporal evolution of the transient (a)  $Nu$ ; (b)  $fRe$  of a wavy channel with  $\alpha = 0.1$ ,  $\beta = 1/2$  and  $\varphi = \pi/3$  within five time periods at  $Re = 200$ .

behavior. Routes by which a flow undergoes transition from steady to chaotic are of fundamental importance and also have wide-ranging engineering applications [32,33]. Transition routes via incommensurate bifurcation (Ruelle–Takens–Newhouse scenario [36,37]), via period-doubling bifurcation (Feigenbaum scenario [38,39]), via intermittency regime (Manneville and Pomeau scenario [40]), or even via hybrid bifurcations [35] have been found for various closed or open flows. The present results show that the transition route to chaotic flow in wavy channels considered in the present study may share some common features with the Ruelle–Takens–Newhouse scenario, via incommensurate bifurcation.

For Reynolds numbers of 366.7 and above, as manifested by the Fourier power spectrum, a chaotic unsteady three-dimensional Eulerian flow field ensues, which is anticipated to give rise to chaotic advection and thus a chaotic flow field when viewed from the Lagrangian viewpoint. This is in contrast to the results in Section 3.1 for low Reynolds numbers of 166.7 and below, where a steady, non-chaotic three-dimensional Eulerian flow field has been dem-

onstrated to exhibit chaotic advection using Poincaré sections and the stretching field associated with Lagrangian fluid particles.

It can be found from the flow field results and discussion in unsteady regimes that the important flow characteristics consist of the spatial and temporal evolution of secondary flow and the loss of flow symmetry. These features may play important roles in generating chaotic advection, enhancing fluid mixing and heat transfer. Heat transfer simulation is carried out with constant wall temperature condition and liquid water ( $Pr = 7$ ) chosen as the coolant. Both the transient and the time-averaged heat transfer performance as well as friction loss of the present wavy channels are studied and compared with straight channels with the same cross sections.

Fig. 19 presents the temporal evolution of the transient Nusselt number  $Nu$  and  $fRe$  of a wavy channel with  $\alpha = 0.1$ ,  $\beta = 1/2$  and  $\varphi = \pi/3$  within five time periods at  $Re = 200$ . The oscillations of these characteristic numbers are typical in unsteady flow regimes. Special attention should be paid to the oscillation of Nusselt number, as the instantaneous low values may result in temporal hot

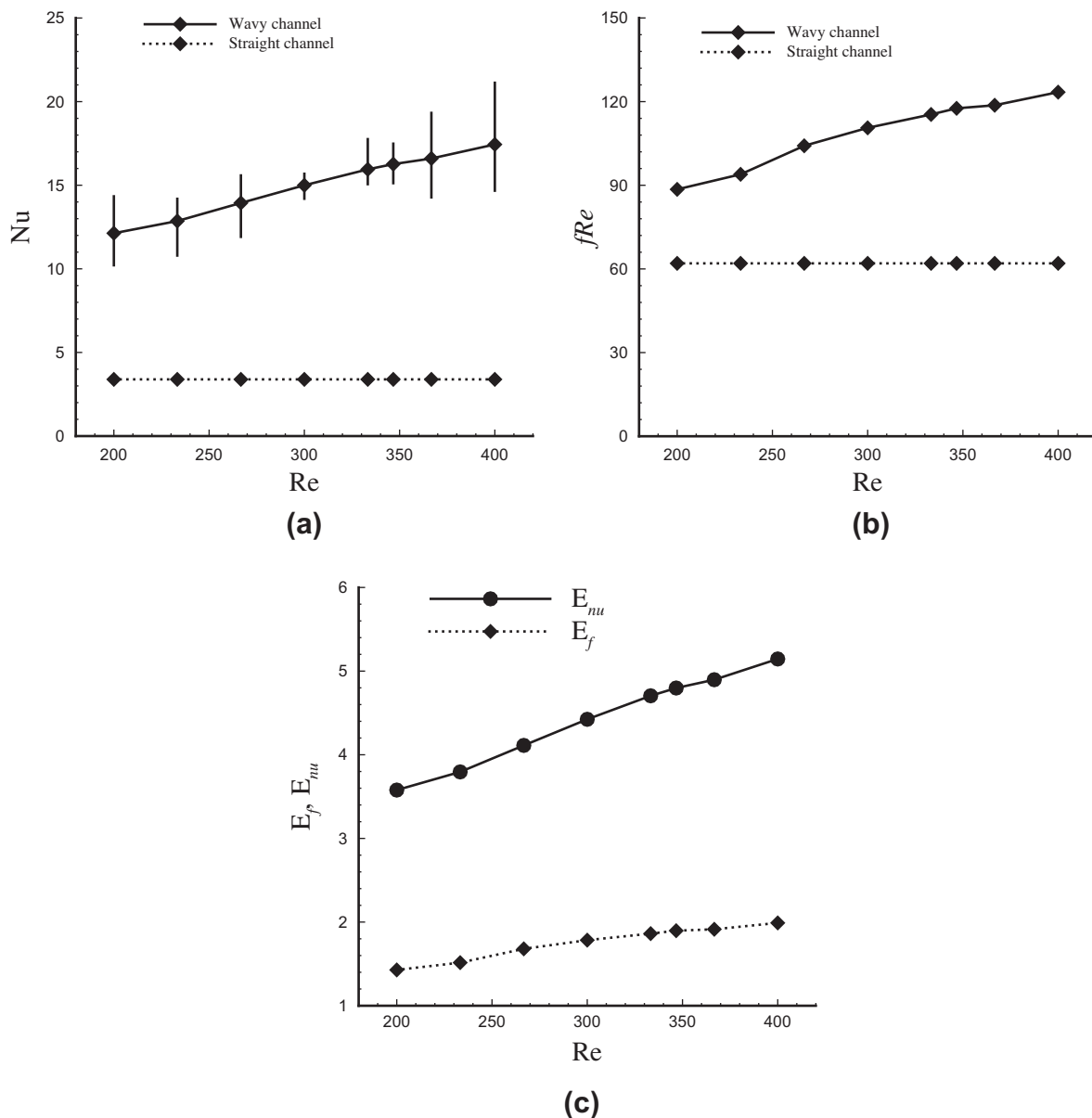


**Fig. 20.** Time-averaged (a)  $Nu$ ; (b)  $fRe$ ; (c) heat transfer enhancement and pressure drop penalty factors of a wavy channel with  $\alpha = 0.1$ ,  $\beta = 1/2$  and  $\varphi = \pi/3$  and a straight baseline channel for different Reynolds numbers. The vertical bold lines in (a) represent the variations in Nusselt number during temporal oscillations.

spots in practical applications. At a certain flow rate (Reynolds number), the friction factor also periodically changes its value at negligibly small oscillation amplitudes, which are within 2% of the average value for all cases considered in the present study. The time-averaged  $Nu$ ,  $fRe$ , heat transfer enhancement and pressure drop penalty factors of a wavy channel with  $\alpha = 0.1$ ,  $\beta = 1/2$  and  $\varphi = \pi/3$  and a straight baseline channel are presented in Fig. 20 for different Reynolds numbers. The vertical bold lines in Fig. 20(a) represent the Nusselt number value regions during oscillation. It can be seen that the heat transfer performance and pressure drop of the present wavy channel monotonically increase with increasing Reynolds numbers, and for all cases considered the heat transfer enhancement is significantly larger than the pressure drop penalty. At  $Re = 400$  which corresponds to chaotic flow, the heat transfer performance is boosted up by 414.5% with a pressure drop penalty increase of only 99.0% compared with straight baseline channel.

When wavy channels are incorporated into heat transfer devices, besides their efficiency in thermal removal ability, another important issue is their compactness. It is obvious that the lower

the wavy amplitude, the greater the compactness. The present simulation also includes wavy channels with smaller rotation angle and thus lower wavy amplitudes. Fig. 21 presents the time-averaged  $Nu$ ,  $fRe$ , heat transfer enhancement and pressure drop penalty factors of a wavy channel with  $\alpha = 0.1$ ,  $\beta = 1/2$ ,  $\varphi = \pi/6$  and a straight baseline channel for different Reynolds numbers. When compared with the results in Fig. 20, it can be confirmed that wavy channels with lower amplitude have lower thermal removal ability and lower pressure drop penalty. However, it can still be found that for all cases considered the heat transfer enhancement is significantly larger than the pressure drop penalty when compared with a straight channel with the same cross section. For example, at  $Re = 400$ , the heat transfer performance is still enhanced by 278.6% with a pressure drop penalty increase of only 51.8% compared with the results of the straight baseline channel. In fact, this good feature persists for all wavy channels considered in the present study. Also, as the wavy amplitude of the present channels is relatively low, they can be nearly as compact as straight channels. Hence, the wavy channels considered in the present study are potentially good candidates for incorporation

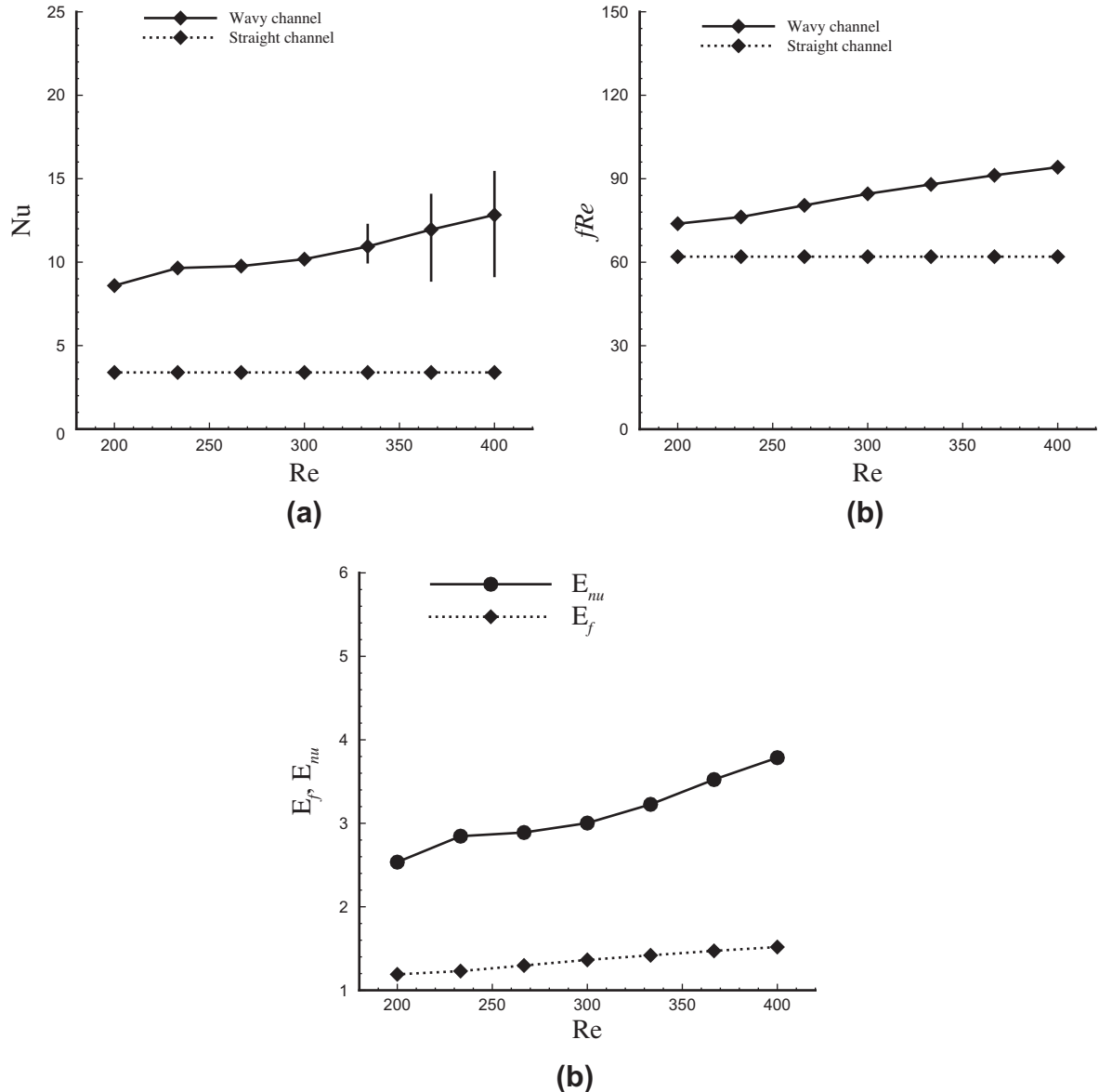


**Fig. 21.** Time-average (a)  $Nu$ ; (b)  $fRe$ ; (c) heat transfer enhancement and pressure drop penalty factors of a wavy channel with  $\alpha = 0.1$ ,  $\beta = 1/2$  and  $\varphi = \pi/6$  and a straight baseline channel for different Reynolds numbers. The vertical bold lines in (a) represent the variations in Nusselt number during temporal oscillations.

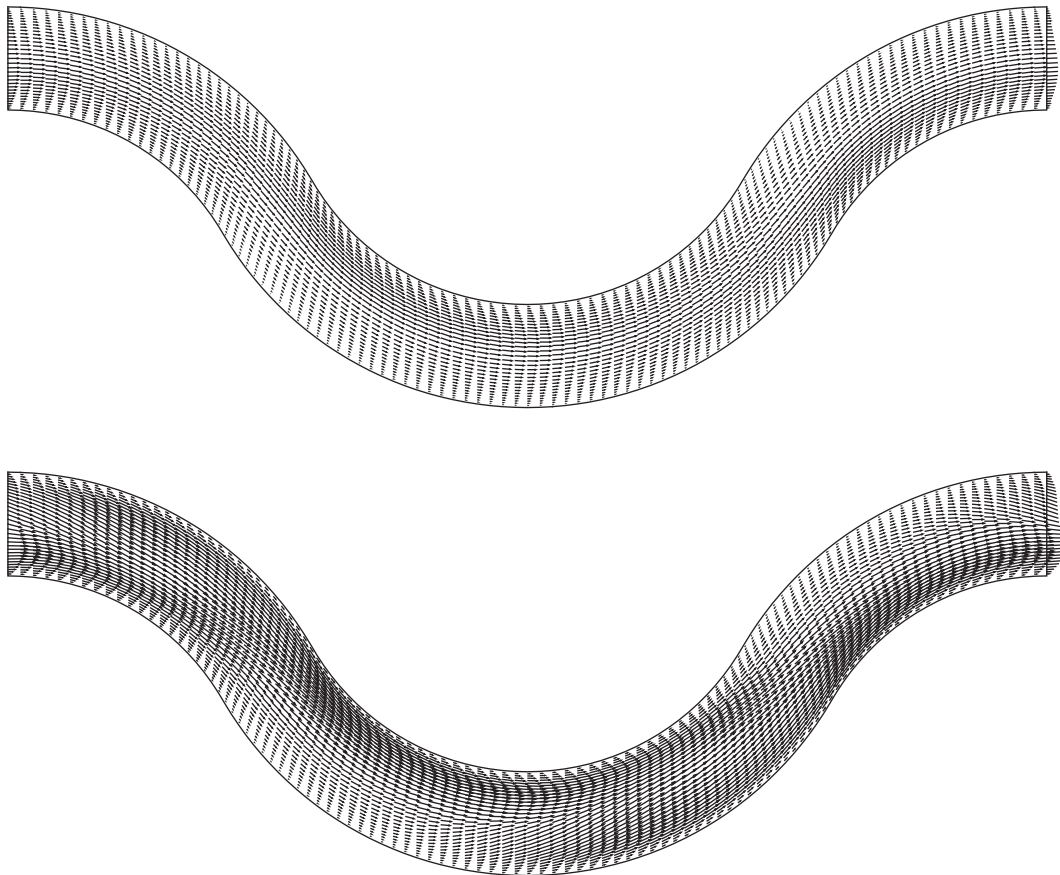


**Fig. 22.** Velocity vectors along the middle cross section ( $z = 0.5H$ ) in  $x$ - $y$  plane of a wavy channel with  $\alpha = 0.1$ ,  $\beta = 1/2$  and  $\varphi = \pi/3$  at  $Re =$  (a) 166.7 and (b) 400.

into various heat transfer devices, such as microchannel heat sinks [41–43].

It should be noted that for flow in wavy channels, there are different mechanisms which are capable of enhancing mixing and heat transfer. For example the curvature induced lateral vortices, which develop in the trough of the wave, have been studied by Metwally and Malik [44], as well as mentioned by Rush et al. [18]. The difference from the present study mainly arises from the different channel geometry considered. The wavy channels in the present study are mainly narrowly spaced and have low relative amplitudes, such that there are no lateral vortices formed, as illustrated in Fig. 22, which presents the velocity vectors along the middle cross section ( $z = 0.5H$ ) in the  $x$ - $y$  plane of a wavy channel with  $\alpha = 0.1$ ,  $\beta = 1/2$  and  $\varphi = \pi/3$  at  $Re = 166.7$  and  $400$ . The heat transfer enhancement in the present wavy channels is mainly due to the enhanced fluid mixing, which is induced by the formation of cross sectional secondary flows and its spatial and temporal evolution.

#### 4. Conclusions

Direct numerical simulation has been carried out to investigate the fully-developed flow and heat transfer in periodic wavy channels with rectangular cross sections. The present study covers the Reynolds number ranging from steady laminar to transitional flow regimes.

Regarding the flow field, the simulation results show that in the steady flow regime, secondary flow (Dean vortices) can develop when liquid coolant passes the channel bends. The patterns of Dean vortices may change significantly along the flow direction,

which can lead to chaotic advection, thus greatly enhancing the convective fluid mixing and heat transfer. Corresponding to an increase in Reynolds number, the flow transits from steady to time periodic with a single frequency, and subsequently to quasiperiodic flow with two incommensurate fundamental frequencies. The flow within these unsteady regimes are characterized by very complex Dean vortices patterns which evolve temporally and spatially along the flow direction, and the loss of flow symmetry. Further increase in Reynolds number leads to aperiodic behavior of the flow and the Fourier spectrum of the velocity evolution becomes broadband and continuous, which suggest chaotic flow. The route to chaos in wavy channels may thus share some common features with the Ruelle-Takens-Newhouse scenario, via incommensurate bifurcation.

For all flow regimes, the corresponding heat transfer simulation is carried out with constant wall temperature condition and liquid water ( $Pr = 7$ ) chosen as the coolant. The results show that due to the efficient mixing in wavy channels, the heat transfer performance can always be significantly better than that of straight channels with the same cross sections; at the same time the pressure drop penalty of wavy channels can be much smaller than the heat transfer enhancement. The wavy channels considered in the present study are efficient and compact, they may have advantages over straight channels and are possibly promising candidates for incorporation into efficient heat transfer devices.

#### Acknowledgement

This research was supported by the Singapore Ministry of Education Academic Research Fund (Tier 1) Grant No. R-265-000-279-112.

## References

- [1] F. Schönfeld, S. Hardt, Simulation of helical flows in micro channels, *AIChE J.* 50 (2004) 771–778.
- [2] F. Jiang, K.S. Drese, S. Hardt, M. Küpper, F. Schönfeld, Helical flows and chaotic mixing in curved micro channels, *AIChE J.* 50 (2004) 2297–2305.
- [3] C.E. Kalb, J.D. Seader, Heat and mass transfer phenomena for viscous flow in curved circular tubes, *Int. J. Heat Mass Transfer* 15 (4) (1972) 801–817.
- [4] J.H. Masliyah, K. Nandakumar, Fully-developed viscous flow and heat transfer in curved semi-circular sectors, *AIChE J.* 25 (3) (1979) 478–487.
- [5] L. Wang, T. Yang, Bifurcation and stability of forced convection in curved ducts of square cross-section, *Int. J. Heat Mass Transfer* 47 (2004) 2971–2987.
- [6] G. Yang, Z.F. Dong, M.A. Ebadian, Laminar forced convection in a helicoidal pipe with fine pitch, *Int. J. Heat Mass Transfer* 38 (5) (1995) 853–862.
- [7] N.R. Rosagutti, D.F. Fletcher, B.S. Haynes, Laminar flow and heat transfer in a periodic serpentine channel with semi-circular crosssection, *Int. J. Heat Mass Transfer* 49 (17–18) (2006) 2912–2923.
- [8] P.E. Geyer, N.R. Rosagutti, D.F. Fletcher, B.S. Haynes, Laminar thermohydraulics of square ducts following a serpentine channel path, *Microfluid. Nanofluid.* 2 (3) (2006) 195–204.
- [9] P.E. Geyer, N.R. Rosagutti, D.F. Fletcher, B.S. Haynes, Laminar flow and heat transfer in periodic serpentine mini-channels, *J. Enhanced Heat Transfer* 13 (4) (2006) 309–320.
- [10] P.E. Geyer, D.F. Fletcher, B.S. Haynes, Laminar flow and heat transfer in a periodic trapezoidal channel with semi-circular crosssection, *Int. J. Heat Mass Transfer* 50 (17–18) (2006) 3471–3480.
- [11] N.R. Rosagutti, D.F. Fletcher, B.S. Haynes, Low Reynolds number heat transfer enhancement in sinusoidal channels, *Chem. Eng. Sci.* 62 (3) (2007) 694–702.
- [12] R.M. Manglik, J. Zhang, A. Muley, Low Reynolds number forced convection in three-dimensional wavy-plate-fin compact channels: fin density effects, *Int. J. Heat Mass Transfer* 48 (8) (2005) 1439–1449.
- [13] Y. Sui, C.J. Teo, P.S. Lee, Y.T. Chew, C. Shu, Fluid flow and heat transfer in wavy microchannels, *Int. J. Heat Mass Transfer* 53 (2010) 2760–2772.
- [14] Y. Sui, C.J. Teo, P.S. Lee, An experimental study of flow friction and heat transfer in wavy microchannels with rectangular cross-section, *Int. J. Thermal Sci.* (2011). doi:10.1016/j.ijthermalsci.2011.06.017.
- [15] L. Gong, K. Kota, W. Tao, Y. Joshi, Parametric numerical study of flow heat transfer in microchannels with wavy walls, *ASME J. Heat Transfer* 133 (2011) 051702.
- [16] H. Aref, Stirring by chaotic advection, *J. Fluid Mech.* 143 (1984) 1–21.
- [17] H. Aref, The development of chaotic advection, *Phys. Fluids* 14 (4) (2002) 1315–1325.
- [18] T.A. Rush, T.A. Newell, A.M. Jacobi, An experimental study of flow and heat transfer in sinusoidal wavy passages, *Int. J. Heat Mass Transfer* 42 (9) (1999) 1541–1553.
- [19] GAMBIT 2.2 User's Guide, 2000, Lebanon, NH, Fluent Inc.
- [20] FLUENT 6 User's Guide, 2000, Lebanon, NH, Fluent Inc.
- [21] R.K. Shah, A.L. London, *Laminar Flow Forced Convection in Ducts*, Academic Press, New York, 1978.
- [22] D.M. Hobbs, F.J. Muzzio, Optimization of a static mixer using dynamical systems techniques, *Chem. Eng. Sci.* 53 (1998) 3199–3213.
- [23] J. Aubin, D.F. Fletcher, C. Xuereb, Design of micromixers using CFD modeling, *Chem. Eng. Sci.* 60 (2005) 2503–2516.
- [24] X.D. Niu, Y.T. Chew, C. Shu, Simulation of flows around an impulsively started circular cylinder by Taylor series expansion- and least squares-based lattice Boltzmann method, *J. Comput. Phys.* 188 (2003) 176–193.
- [25] J.M. Ottino, *The Kinematic of Mixing: Stretching, Chaos and Transport*, Cambridge University Press, New York, 1989.
- [26] J.M. Ottino, Mixing, chaotic advection and turbulence, *Ann. Rev. Fluid Mech.* 22 (1990) 207–253.
- [27] A.D. Stroock, S.K.W. Dertinger, A. Ajdari, I. Mezic, H.A. Stone, G.M. Whitesides, Chaotic mixer for microchannels, *Science* 295 (2002) 647–651.
- [28] H.M. Xia, S.Y.M. Wan, C. Shu, Y.T. Chew, Chaotic micromixers using two-layer crossing channels to exhibit fast mixing at low Reynolds numbers, *Lab Chip* 5 (2005) 748–755.
- [29] H.M. Xia, S.Y.M. Wan, C. Shu, Y.T. Chew, Influence of the Reynolds number on chaotic mixing in a spatially periodic micromixer and its characterization using dynamical system techniques, *J. Micromech. Microeng.* 16 (2006) 53–61.
- [30] C. Chagny, C. Castelain, H. Peerhossaini, Chaotic heat transfer for heat exchanger design and comparison with a regular regime for a large range of Reynolds numbers, *Appl. Thermal Eng.* 20 (2000) 1615–1648.
- [31] Y. Lasbet, B. Auvity, C. Castelain, H. Peerhossaini, A chaotic heat-exchanger for PEMFC cooling applications, *J. Power Sources* 156 (2006) 114–118.
- [32] G.E. Karniadakis, G.S. Triantafyllou, Three-dimensional dynamics and transition to turbulence in the wake of bluff objects, *J. Fluid Mech.* 238 (1992) 1–30.
- [33] A.M. Guzmán, C.H. Amon, Dynamical flow characterization of transitional and chaotic regimes in converging diverging channels, *J. Fluid Mech.* 321 (1996) 25–57.
- [34] A.M. Guzmán, M.D. Valle, Heat transfer enhancement in grooved channels due to flow bifurcations, *Heat Mass Transfer* 42 (2006) 967–975.
- [35] J. Zhang, N.S. Liu, X.Y. Lu, Route to a chaotic state in fluid flow past an inclined flat plate, *Phys. Rev. E* 79 (2009) 045306.
- [36] D. Ruelle, F. Takens, On the nature of turbulence, *Commun. Math. Phys.* 20 (1971) 167–192.
- [37] S. Newhouse, D. Ruelle, F. Takens, Occurrence of strange axiom A attractors near quasiperiodic flow on  $T^m$ ,  $m \geq 3$ , *Commun. Math. Phys.* 64 (1978) 35–40.
- [38] M. Feigenbaum, The transition to aperiodic behavior in turbulent systems, *Commun. Math. Phys.* 77 (1980) 65–86.
- [39] T.H. Pulliam, J.A. Vastano, Transition to chaos in an open unforced 2D flow, *J. Comput. Phys.* 105 (1993) 133–149.
- [40] P. Manneville, Y. Pomeau, Different ways to turbulence in dissipative dynamical systems, *Physical D* 1 (1980) 219–226.
- [41] D.B. Tuckerman, R.F.W. Pease, High-performance heat-sinking for VLSI, *IEEE Electron. Dev. Lett.* 2 (5) (1981) 126–129.
- [42] I. Hassan, P. Phutthavong, M. Abdalgawad, Microchannel heat sinks: an overview of the state-of-the-art, *Microscale Thermal Eng.* 8 (2004) 183–205.
- [43] S.V. Garimella, C.B. Sobhan, Transport in microchannels – A critical review, *Annu. Rev. Heat Transfer* 13 (2003) 1–50.
- [44] H.M. Metwally, R.M. Manglik, Enhanced heat transfer due to curvature-induced lateral vortices in laminar flows in sinusoidal corrugated-plate channels, *Int. J. Heat Mass Transfer* 47 (10–11) (2004) 2282–2292.